




Magnetic Field and Electron Density Anomalies from Swarm Satellites Preceding the Major Earthquakes of the 2016–2017 Amatrice-Norcia (Central Italy) Seismic Sequence

DEDALO MARCHETTI,^{1,2}  ANGELO DE SANTIS,^{2,4} SERENA D'ARCANGELO,³ FEDERICA POGGIO,⁴ SHUANGGEN JIN,¹
ALESSANDRO PISCINI,² and SAIOA A. CAMPUZANO²

Abstract—A systematic inspection of the magnetic field and electron density, recorded by Swarm three-satellite constellation over the seismic region hit by the 2016–2017 Amatrice-Norcia (Central Italy) seismic sequence, has allowed us to identify some possible precursory anomalies, when disturbed periods of the geomagnetic conditions are properly taken into account and/or avoided. This paper aims at studying and interpreting the electromagnetic phenomena occurred before and during the 2016–2017 Amatrice-Norcia (Central Italy) seismic sequence, in order to look for any possible evidence of precursory anomalies. Results show magnetic field and electron density anomalies of four tracks that precede the major earthquakes of the seismic sequence. After an inspection of the geomagnetic conditions, a Swarm Charlie track, acquired on 20/08/2016 that precedes by 3.2 days the beginning of the whole seismic sequence, remains unexplainable with the normal geomagnetic disturbance phenomena of the Earth's magnetic field. Furthermore, we carry out a blind study of possible relationship between abnormal magnetic field signals detected by Swarm satellites during geomagnetic quiet conditions and major seismic events from about 4 months before the start of the seismic sequence until about the first 8 months from the seismic sequence (i.e. a total of one year of analysed data). We find a very interesting increase of such anomalies starting about 40 days before the beginning of the seismic sequence. It coincides and follows surface and atmospheric alterations, resulting in a temporal sequence of anomalies from Earth's surface up to ionosphere, supporting the possibility of lithosphere–atmosphere–ionosphere coupling models.

Key words: Seismo-magnetic precursors, LAIC, Swarm satellites, earthquakes.

1. Introduction

The main purpose of this paper is to look for possible evidence, in terms of abnormal electromagnetic measurements, of the influence in the ionosphere by the earthquakes in a specific case study. These phenomena are called Lithosphere Atmosphere Ionosphere Coupling (LAIC) effects.

Different models have been proposed to explain the possible LAIC effects in the atmosphere and in the ionosphere. Freund (2011, 2013) proposed a mechanism based on the theory of p-holes (positive holes), considering the Earth crust as a battery. The stress along the fault produces p-holes which alter the surrounding rocks producing electric current and, suddenly, electromagnetic radiations and pulses. When p-holes reach the Earth surface they could ionize the atmosphere and, rising upward, could then lead to cloud condensation. The upward of these charged particles could create instability in the mesosphere and on the edge of the ionosphere. The mechanisms were tested successfully in laboratory as reported in Freund et al. (2007).

Pulinets and Ouzounov (2011) proposed a slightly different model to explain the LAIC effects, based mainly on gas and fluid that could rising up toward the surface in the preparatory phase of the earthquake. Some evidence for underground fluids migration were also provided by seismological analysis, for example for Central Italy L'Aquila 2009 earthquake by Di Luccio et al. (2010). The surface release of gas could create a chain of processes, among all: a change in surface temperature and humidity, the ionization in atmosphere by alpha-particles, formation of aerosol size particles, changes

¹ School of Remote Sensing and Geomatics Engineering, Nanjing University of Information Science and Technology, Nanjing 210044, China. E-mail: dedalo_marchetti@yahoo.it; 002990@nuist.edu.cn

² Istituto Nazionale di Geofisica e Vulcanologia, Via di Vigna Murata, 605, 00143 Rome, Italy.

³ Facultad Física, Univ. Complutense de Madrid, Avd. Complutense, s/n, 28040 Madrid, Spain.

⁴ Università Gabriele D'Annunzio, Chieti, Italy.

in atmospheric electric conductivity and electric coupling with ionosphere creating electrical and magnetic alterations.

A very interesting LAIC model together with numerical simulation was provided by Kuo et al. (2014). This model is focused on the electromagnetic coupling between lithosphere, atmosphere and ionosphere. It also takes into consideration the role of the Earth's magnetic field, suggesting a possible mechanism of alteration of the ionosphere that improves their previous model published in Kuo et al. (2011).

De Santis et al. (2015) suggested a general review of the processes that occur before and during an intense earthquake, and described how they could be likely coupled. Pulnets and Boyarchuk (2004) and Hayakawa (2015) presented very good general reviews about possible effects in ionospheric plasma density alteration before an earthquake.

Other studies proposed passive ground-based measurements of electromagnetic lithospheric emissions ranging from DC to VHF before M6.9 1988 Spitak (Armenia), M7.1 1989 Loma Pietra (USA) and other earthquakes (Fraser-Smith 1990; Molchanov et al. 1992; Donner et al. 2015).

Hattori (2004) provided a review about different reported pre-earthquake anomalies in ULF geomagnetic field range as one of the most promising phenomena for short-term prediction.

De Santis et al. (2017) applied a specific technique based on the critical system theory to the M7.8 2015 Nepal earthquake taking advantage of the Swarm satellite mission composed of three twin satellites with the main aim of monitoring and studying the Earth's geomagnetic field. These authors found out a particular pattern in the sequence of magnetic anomalies characterised by a great similarity with the analogous foreshocks and aftershocks sequence. A similar approach was applied to the M7.8 2016 Ecuador and M8.2 2017 Mexico earthquakes by Akhoondzadeh et al. (2018) and Marchetti and Akhoondzadeh (2018), finding an increase in the number of Swarm anomalies around 9 days and 130 days, respectively, before the earthquake origin time and other anomalies both in the magnetic field and in the atmosphere and the ionosphere.

In this paper, we aim to analyse both the magnetic field and electron density in situ measurements by

ESA Swarm satellite constellation preceding the major earthquakes of the 2016–2017 Amatrice-Norcia (Central Italy) seismic sequence. In the next section, we describe the seismological context, while in the Sect. 3 we introduce the Swarm satellites together with the used algorithms. Section 4 shows the obtained results, Sect. 5 is dedicated to a blind research for magnetic anomalous signal, and in Sect. 6 we discuss the results, together with some conclusions.

2. Seismological Settings

On 24/08/2016 at 01:36 UTC, a Mw 6.0 earthquake occurred in Central Italy Apennines (42.7 N, 13.23 E, depth of 8 km), 1 km West from Accumoli (Rieti) and 9 km from Amatrice (Rieti) (Tinti et al. 2016). Both towns (and many others in the surrounding) were sadly destroyed, producing about 300 fatalities.

Following this event, a very long seismic sequence started (geographical representation in Fig. 1). In the first year, it produced:

- 2 M6+ earthquakes,
- 7 earthquakes with $5.0 \leq M \leq 5.9$,
- 62 earthquakes with $4.0 \leq M \leq 4.9$,
- 1073 earthquakes with $3.0 \leq M \leq 3.9$,
- more than 75,000 earthquakes with $M \leq 2.9$.

On 30/10/2016, at 6:40 UTC, the Mw 6.5 main shock happened, 5 km Nord-East from Norcia (Perugia) (black-orange star in Fig. 1). On 18/01/2017, a further increase in seismicity occurred, with four Mw 5.0+ events with epicenters close to Montetereale in the region of Campotosto, representing the southernmost part of the sequence.

3. Satellite Swarm Data and Analysis

Swarm is the ESA's magnetic field mission launched successfully on 22/11/2013, which monitors the Earth's magnetic field with a precision never reached before. Some of the principal results obtained so far by Swarm mission are: the lithospheric magnetic field map with a resolution up to 250 km (Olsen

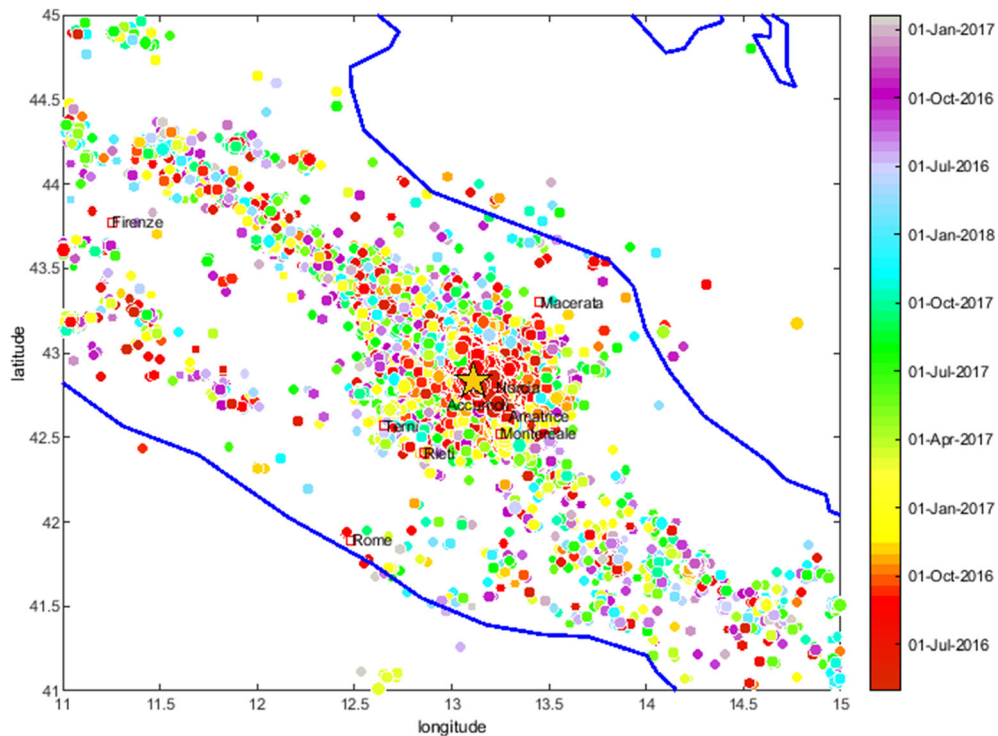


Figure 1

Location of the epicenters, localized by Istituto Nazionale di Geofisica e Vulcanologia (INGV) from 24/08/2016 to 31/12/2017. The size of the points is proportional to the earthquake magnitude while the color indicates the origin time of the event (see the colorbar for a correspondence). Looking at the color it is possible to distinguish in red the initial events close to M6.0 Amatrice, in yellow the events linked to the M6.5 mainshock (black–orange star) close to Norcia and in green the events of the last southern part of seismic sequence, close to Montoneale (Campotosto)

et al. 2017), oceanic tidal effect on geomagnetic field and electromagnetic induction generated by oceanic circulation (e.g. Grayver et al. 2016; Irrgang et al. 2017; Lück et al. 2018).

Swarm is a constellation of three identical satellites, which are still in orbit (Friis-Christensen et al. 2006). Two satellites, Alpha and Charlie are on a lower orbit [about 450 km above sea level (a.s.l.) in August 2016] and the third satellite Bravo is on higher orbit (about 512 km a.s.l. in August 2016). This particular orbital configuration was chosen to achieve many different scientific objectives, for example the side-to-side flight of the two satellites Alpha and Charlie could permit to measure the Field Aligned Currents (FAC) that flow about in radial direction (Ritter et al. 2013). The configuration is not completely fixed as the Bravo satellite precedes slowly in longitude along the years with respect to the other two satellites: at the launch it was close to

Alpha and Charlie, now it is about at 90° separation. Also the altitude is an important parameter as it was chosen to extend the mission, maintaining by fuel the altitude of Alpha and Charlie that are more subject to drag. In this way, it will be possible to monitor the geomagnetic field for an entire solar cycle (11 years) and this is very important as the Solar physics plays one of the most important impacts on geomagnetic field, in fact also in this study, to search for seismic source anomalies we try to be in conditions that are as less perturbed as possible by external sources like the Sun.

The satellites are equipped by sophisticated magnetometers to acquire vector magnetic field and its intensity, electric field instruments to characterise the ionospheric plasma, accelerometers and other tools, as laser retroreflectors to determine the orbit in a very accurate way.

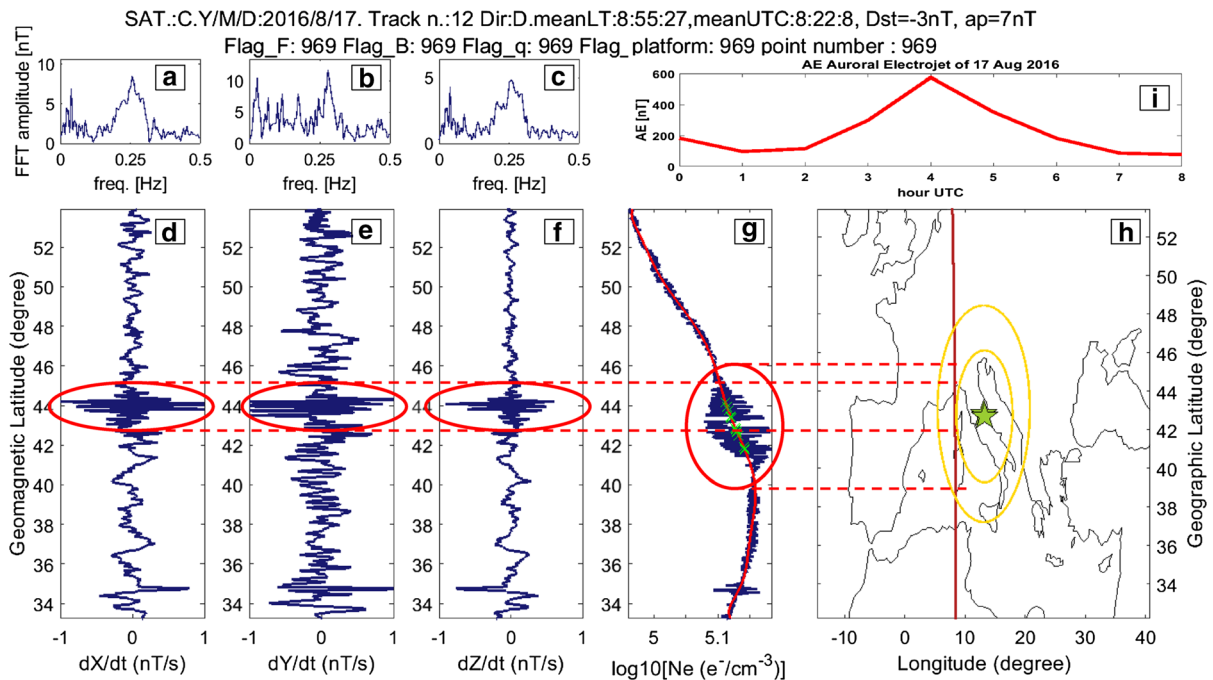


Figure 2

Swarm magnetic and electron density signals corresponding to track no. 12 of the 17/08/2016. The small plot at the top right represents the AE-index in the same day preceding the shown track. Red circle underlines an anomaly on all the vector components of magnetic field and the plasma electron density

The geomagnetic field is measured by two instruments: Absolute Scalar Magnetometer (ASM) and Vector Field Magnetometer (VFM), which are placed at the end and at the half of the 4 m boom, respectively, both placed at the back of each satellite. The electronic boards are placed inside the satellite main body, as much as farther from the sensors. The ASM works on the physics principle of measuring the Larmor frequency of ^4He in one of its metastable levels, which obviously depends on the magnetic field environment where the sensor is placed. The ASM characteristic errors are significantly lower than 1 nT (Léger et al. 2015). Unfortunately, the ASM instrument on-board Swarm Charlie was subject to failure and was off from 5 November 2014. The VFM is composed by a fluxgate magnetometer based on a three-axis Compact Spheric Coil with a three-axis Compact Detector Coil inside. The continuous calibration of the instrument is provided by ASM instrument of the same spacecraft or Alpha ASM for Charlie VFM. The Vector Field Instrument is placed on an optical bank together with

three star trackers to determine with very high precision the absolute orientation of the instrument also in case of deformation and/or vibration of the boom with respect to the spacecraft main body. Joint together the star tracker and the VFM have also permitted to achieve a very high accuracy, comparable with the 4 nT rms of Magsat satellite (see Olsen et al. 2010). In front of each Swarm spacecraft, two Langmuir Probe of different length are installed. A bias electric signal is injected into the probe, but they do not operate by the classic electric sweep cycle, but with an harmonic modulation of the bias at three relevant points to determine the plasma parameters, i.e. the electron density, temperature and potential as reported by Knudsen et al. (2017).

In this paper, the Level 1b magnetic and electric field instrument (EFI) dataset are analysed. Detailed corresponding official description can be found in Olsen et al. (2013). For magnetic field we analyse the Low Resolution 1 Hz version 408 data. Electron density is extracted from EFIx_LP 2 Hz, version 403 data.

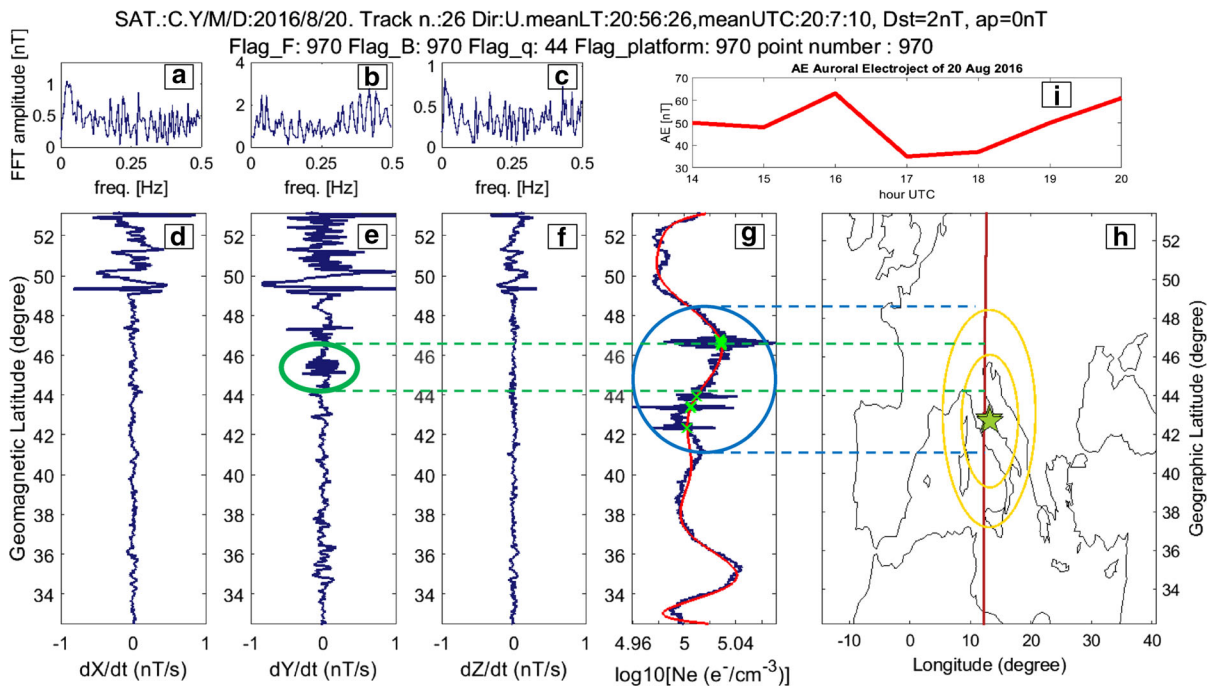


Figure 3

Anomalous track of Swarm Charlie satellite in magnetic and electron density recorded 3.2 days before the M6.0 Amatrice earthquake (24/08/2016). Green and blue circles highlight very interesting anomalies in magnetic field and electron density, respectively

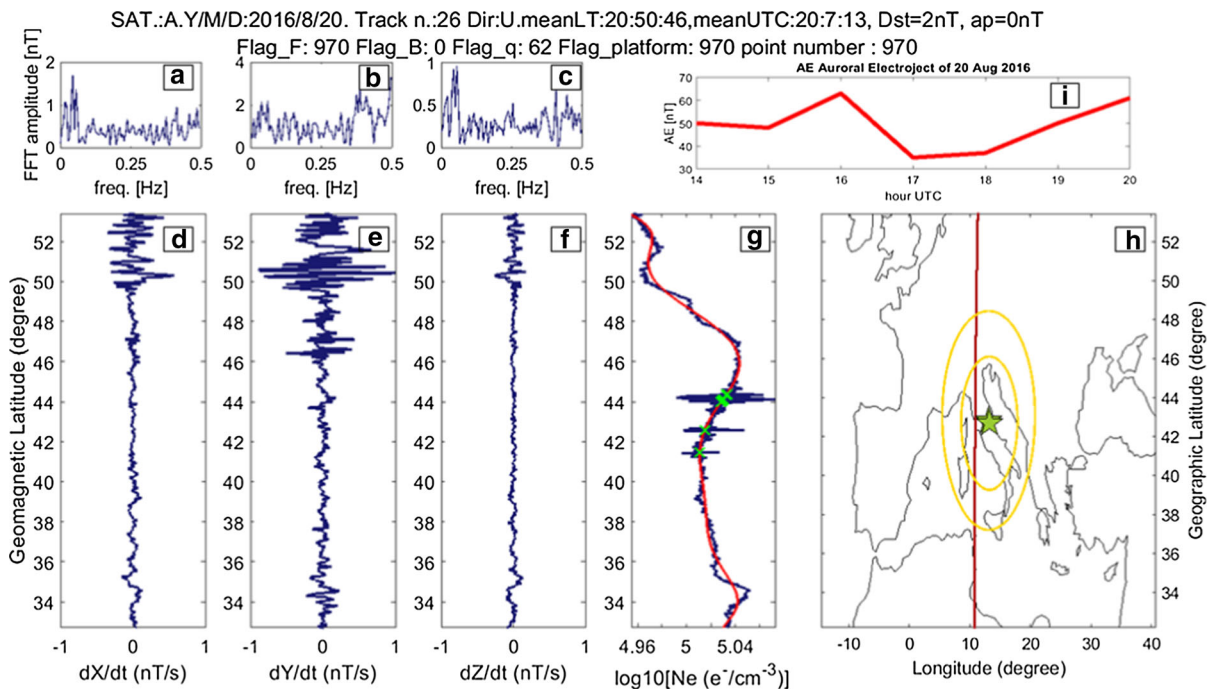
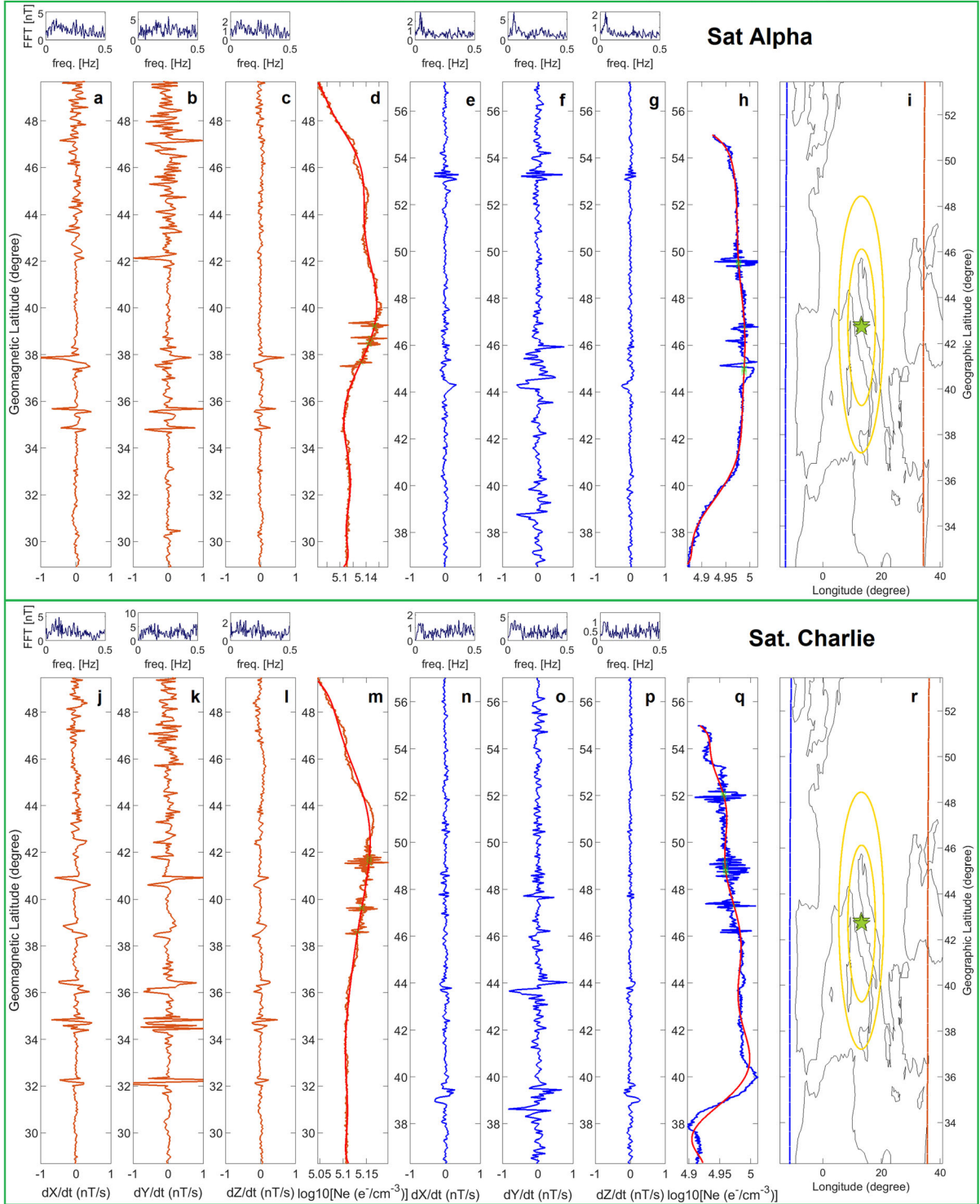


Figure 4

Swarm Alpha satellite magnetic and electron density signals of track no. 26 acquired on 20/08/2016. The track is shown to be compared with Fig. 3 as Alpha satellite crosses the same region after 3.2 s with respect to Charlie

SAT.:A&C.Y/M/D:2016/8/20

Track n.:24. meanLT:20:54,meanUTC:18:33, Dst=2nT, ap=0nT - Track n.:29. meanLT:20:53,meanUTC:21:41, Dst=-3nT, ap=4nT



◀Figure 5

Alpha and Charlie Swarm magnetic and electron density satellite tracks that precede and follow the tracks of 20/08/2016 of Figs. 3 and 4 (see main text for more details)

In Figs. 2, 3, 4, 5, 6 and 7 we show the results of semi-automatic data analysis over the three magnetic field components, the total intensity, the electron density and the geographical map (from left to right). For each component of the magnetic field, we extract the measurements in the latitude between about 33° N and 53° N (geographical latitude). The magnetic latitude (by rotation taking into account North Pole by IGRF-12, Thébault et al. 2015), the central track UTC time and the corresponding local time for that longitude λ ($LT = UT + \lambda/15$) are computed and shown in output graphs. The magnetic data are elaborated to remove the main field with the same approach described in De Santis et al. (2017). Therefore, we calculate the differences sample by sample divided by the time difference of two

consecutive samples (that, numerically, it approximates the temporal derivative) and then we remove a cubic spline with knock points every 20 s from the data in order to remove the long trend of the time series. Next, residuals are plotted and investigated. The scale is fixed in the range ± 1 nT/s, so that it can be possible to compare the residual of a particular track to another (sub-pictures d, e and f). The decimal logarithm of electron density is also plotted in sub-picture g and analysed. In order to identify the possible outliers, a 10° polynomial is fitted over the electron density and is represented in the next figures as a red curve. The electron density's samples, which deviate more than 2.0 times from the standard deviation of the residual of the polynomial fit, are automatically highlighted by a green "X". On the sub-picture h, a geographical map allows to see the localization of the studied area, marked by a yellow circle that defines the Dobrovolsky area of the mainshock, with a radius of about 620 km (Dobrovolsky et al. 1979). In some graphs, we represent also the M6.0 Amatrice earthquake's Dobrovolsky area of

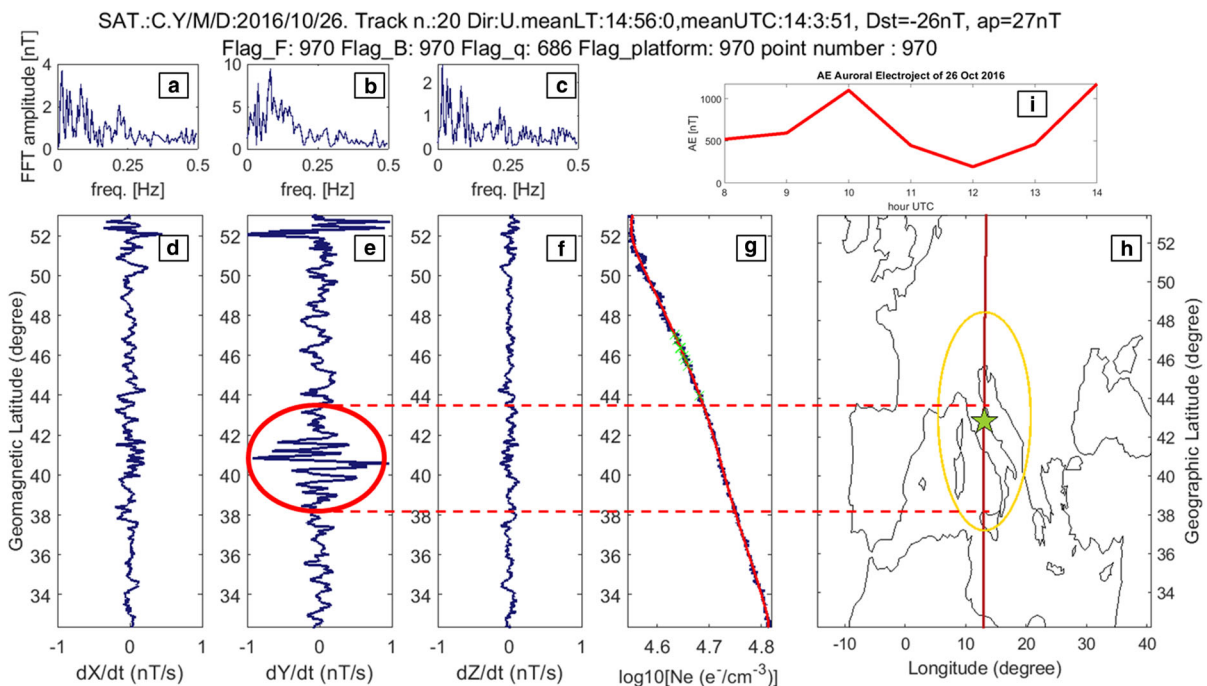


Figure 6

Swarm Charlie magnetic and electron density tracks no. 20 of the 26/10/2016. The track precedes by 3 h the Mw 5.4 and by 5 h and 15 min the Mw 5.9 earthquakes of the same day and by 3 days, 16 h and half the 30/10/2016 Mw 6.5 mainshock

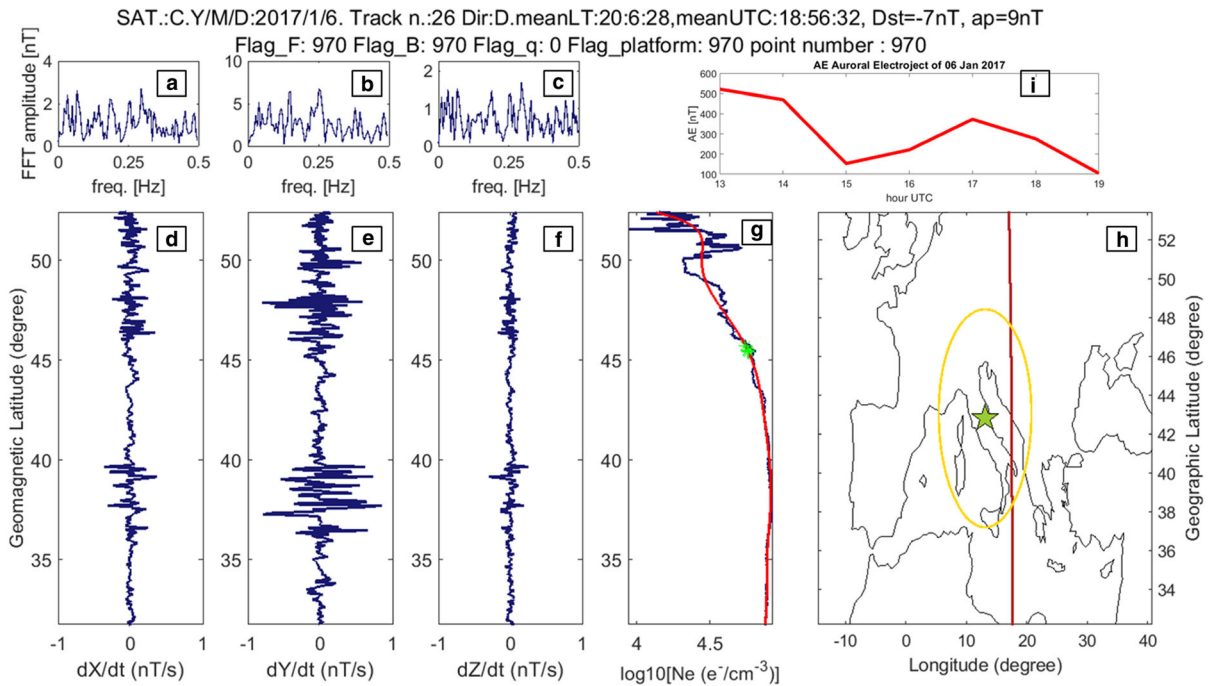


Figure 7

Swarm Charlie magnetic and electron density signals along the track no. 26 of the 06/01/2017

about 380 km. Other elements in the geographical map are: a red line, representing the studied satellite track, and a green star as the mainshock epicenter. All the plots referring to the same figure have been aligned at the same latitude and time; the geomagnetic latitude is also represented. Each of the three components of the magnetic field is also given with its Fast Fourier Transform (FFT) in subpictures a, b and c for X, Y and Z geomagnetic residual, respectively. The samples inside the minimum and maximum latitude of the Dobrovolsky circle are taken into account for FFT estimation. As the number of the samples influences the FFT results and overall the sensibility at different periods we decide to fix the same limits for all the tracks at every longitude. In the head of figure, we also report title, day and mean hour, geomagnetic conditions (Dst, a_p geomagnetic indices values during the acquisition time and AE index for previous 6 h), satellite quality flags and satellite flight direction (Dir: U for Up-ascending or D for Down-descending orbit).

A total automatic and blind data analysis is presented in Fig. 9 and Sect. 5 of this paper. The analysis

is conducted with the best results of the previous investigation and introducing also a continuous wavelet analysis over 1 year of Swarm data. In particular, we write an algorithm that investigates each satellite track that crosses the Dobrovolsky area and compares the root mean square inside a small (1°) moving window with the root mean square of the whole track. On the same time, the algorithm performs the wavelet analysis and it estimates the energy content inside the signal period of 40–60 s. If it detects in the same moment a high root mean square and high frequency content it tags that track as anomalous. The details are provided in Sect. 5. The advantage of this technique is that the anomaly is defined by objective criteria, without human interaction.

4. Results and Analysis

Firstly, starting from 1 month before the beginning of the seismic sequence to the end of January 2017, the graphs of all the satellite tracks of Alpha, Bravo and Charlie that cross the Dobrovolsky area

are produced. The adjacent tracks, falling outside the Dobrovolsky area, are also analysed, so that a better understanding of any other phenomena is possible. If the same peculiarities of a track, inside of the Dobrovolsky area, are found outside, that track is rejected as a potential earthquake-related anomaly. In total, over 1500 tracks are one-by-one investigated.

In the following lines, we will discuss the tracks evidencing some peculiar features that precede the major shocks of the seismic sequence.

Figure 2 shows a track by Charlie Swarm Satellite acquired on 17/08/2016. The geomagnetic conditions during the hour of the track acquisition time are very quiet ($Dst = -3$ nT, $a_p = 4$ nT, $AE = 76$ nT). The track precedes by 6.7 days the first major earthquake of the sequence. The anomaly highlighted in red could have been good candidate as earthquake precursor, but it is probably due to the decreasing phase in the strong auroral activity, that took place about 4 h earlier (see sub-plot “i” in the same figure), reaching the maximum measured value of AE equal to 576 nT at 4:00 UTC. So, despite the geomagnetic indices correspond to a quiet condition, probably the ionosphere remained still perturbed by the previous activity. It is well known that auroral activity can also be transmitted to medium latitudes (those in this study), generally with delays up to 6 h (Kikuchi et al. 2000).

Figure 3 shows the magnetic field and electron density tracks of Swarm Charlie satellite that passes close to the epicenter 3.2 days before the start of the seismic sequence. The track is acquired at 20:07 UTC on the 20/08/2016 in very quiet geomagnetic conditions ($Dst = 8$ nT, $a_p = 0$ nT, $AE = 50$ nT) and it allows to see a clear anomaly, marked with a green circle, in the Y magnetic component within the Dobrovolsky area, a little northern from the impending earthquake epicenter. In addition, the electron density measured by EFI instrument (Langmuir Probe) onboard the same satellite shows a more extended anomaly, which covers from the southern part to the northern one with respect to the future epicenter; the anomaly is marked with a blue circle. Despite the previous and following tracks (see Fig. 5) present some oscillations of the signal that seem typical of some little external disturbance, they do not present this kind of behaviour, hence, it appears as a

unique feature above the epicentral region. The corresponding track of Alpha satellite (see Fig. 4) presents a disturbance over $+50^\circ$ geomagnetic latitude probably due to the fact that the auroral activity is not totally absent (AE is equal to 50 nT). At 46° geomagnetic latitude, Alpha satellite measures a little disturbance in Y component. The time separation between Alpha and Charlie at that latitude is 3.15 s (with Charlie in front) so the disturbance highlighted with a green circle, in Fig. 3, is a quick transient hiding for the most part after 3 s. Referring to the electron density, the wide blue disturbance is also present in Alpha measurements and in the other tracks of the day in neighbouring regions (but with different peculiarities). They can be identified with about three electron density stronger peaks in all the tracks but the extension along the track and intensity are not the same. The perturbation detected by Charlie satellite in green circle (panel e) in magnetic Y component, probably, is present also in electron density but it is very difficult or impossible to distinguish from the biggest general perturbation of electron density that is likely due to external perturbation. The magnetic signal detected by Charlie satellite in the Y component of the magnetic field could be strongly connected with the impending earthquake and, more important, can be a very good candidate to represent a magnetic precursor, remembering that the 24/08/2016 Mw 6.0 Amatrice earthquake was not preceded by foreshocks.

Looking at the residual magnetic satellite signals over Central Italy Apennines, we notice an abnormal track at around the 26 October, as shown in Fig. 6, which is clearly different from the other ones.

This track precedes by about 3.7 days the Mw 6.5 mainshock happened at 6:40 UTC on 30/10/2016 close to the town of Norcia. The anomaly is marked with a red circle and it appears even before two foreshocks, i.e. 3 h before the Mw 5.4 and 5 h and 15 min before the Mw 5.9 earthquakes, occurred on the same day of the satellite track. A very deep earthquake (depth 481 km) of magnitude ML 5.8 also occurred after 54 h (i.e. 28/10/2016 20:02:43 UTC) in Southern Tyrrhenian Sea (39.27 N, 13.55 E), but we do not expect it produced this anomaly as being a very deep earthquake. Geomagnetic conditions during which we acquire this track show a moderate activity ($Dst = -26$ nT, $a_p = 27$ nT). The corresponding

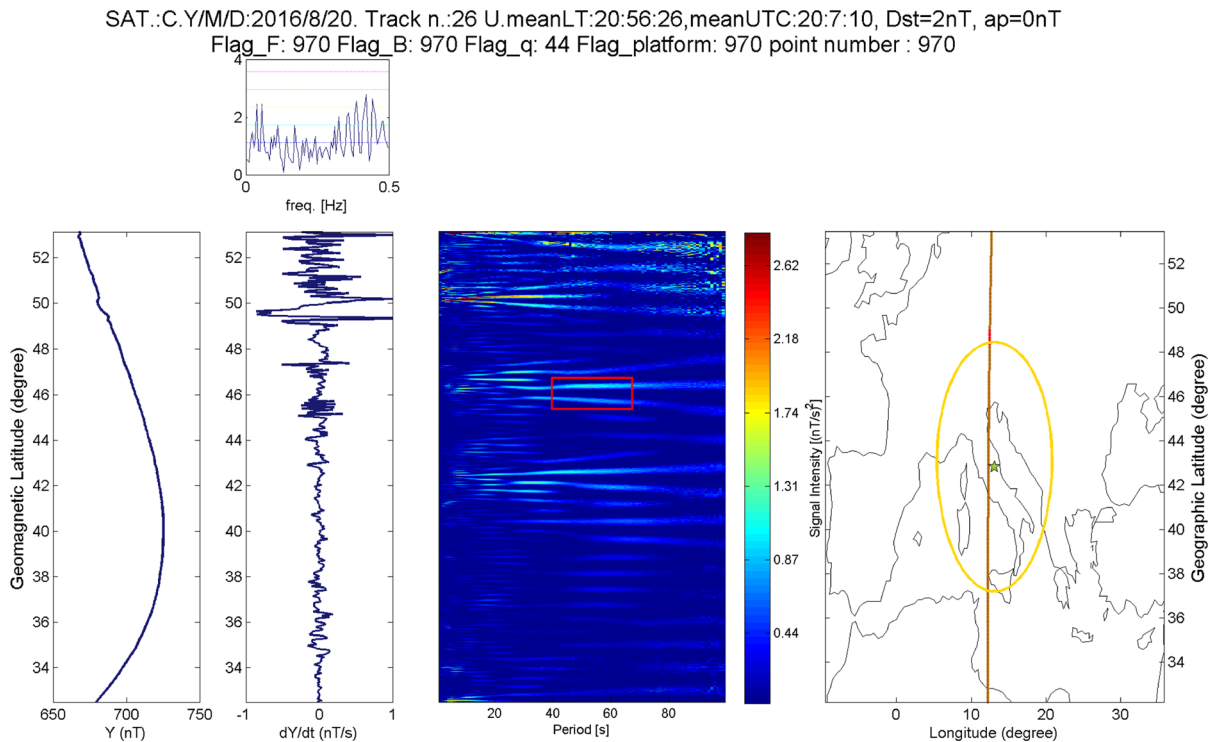


Figure 8

Swarm Charlie Y component magnetic signals along the track no. 26 acquired at 20:07 UTC of the 20/08/2016. In the figure is represented (from left to right) the original signal, the residual of removing cubic spline from the first derivative and the continuous wavelet analysis in the period between 2 and 100 s

Y-component track has a particular period of oscillation, also highlighted by the peak in the Fourier transform at about 13 s that exceeds by 3 sigmas the average of the spectrum. Measuring the peak-to-peak amplitude manually on the graph for the abnormal signals, we estimate a characteristic time in the range 7–11 s. The signal then shows an increase of the central frequency.

If we suppose that the phenomenon can be ascribed to a “Doppler effect”, this should be induced from a front of particles moving at speed equal to about 57% of the light speed.

In the days preceding the 18/01/2017 (when occurred four M5+ seismic events located near Montereale, in the Campotosto area), unfortunately both magnetometers onboard Alpha and Charlie satellites were not in nominal conditions. The only track with a clear anomaly and nominal working condition of satellite instruments was acquired by Swarm Charlie on 6/01/2017 at 18:56 UTC (Fig. 7). The

auroral activity throughout the whole day was high: during the acquisition of this track we find AE (19:00 UT) = 104 nT; please note that 6 h before this track, the AE-index reached even the highest value of the day, i.e. 521 nT. Therefore, the anomalies found in this track are more probably due to the penetration of auroral electric currents at medium latitudes than precursors.

5. Validation of the Visual Inspection of the Satellite Tracks

After the visual inspection of the tracks together with an investigation of the geomagnetic conditions before and during the 2016–2017 Central Italy seismic sequence, the Charlie track no. 26 acquired on 20 August at 20:07 UTC can be considered as a good seismic precursor candidate.

Specific frequency analysis on this track by continuous wavelet Morlet family is performed. The

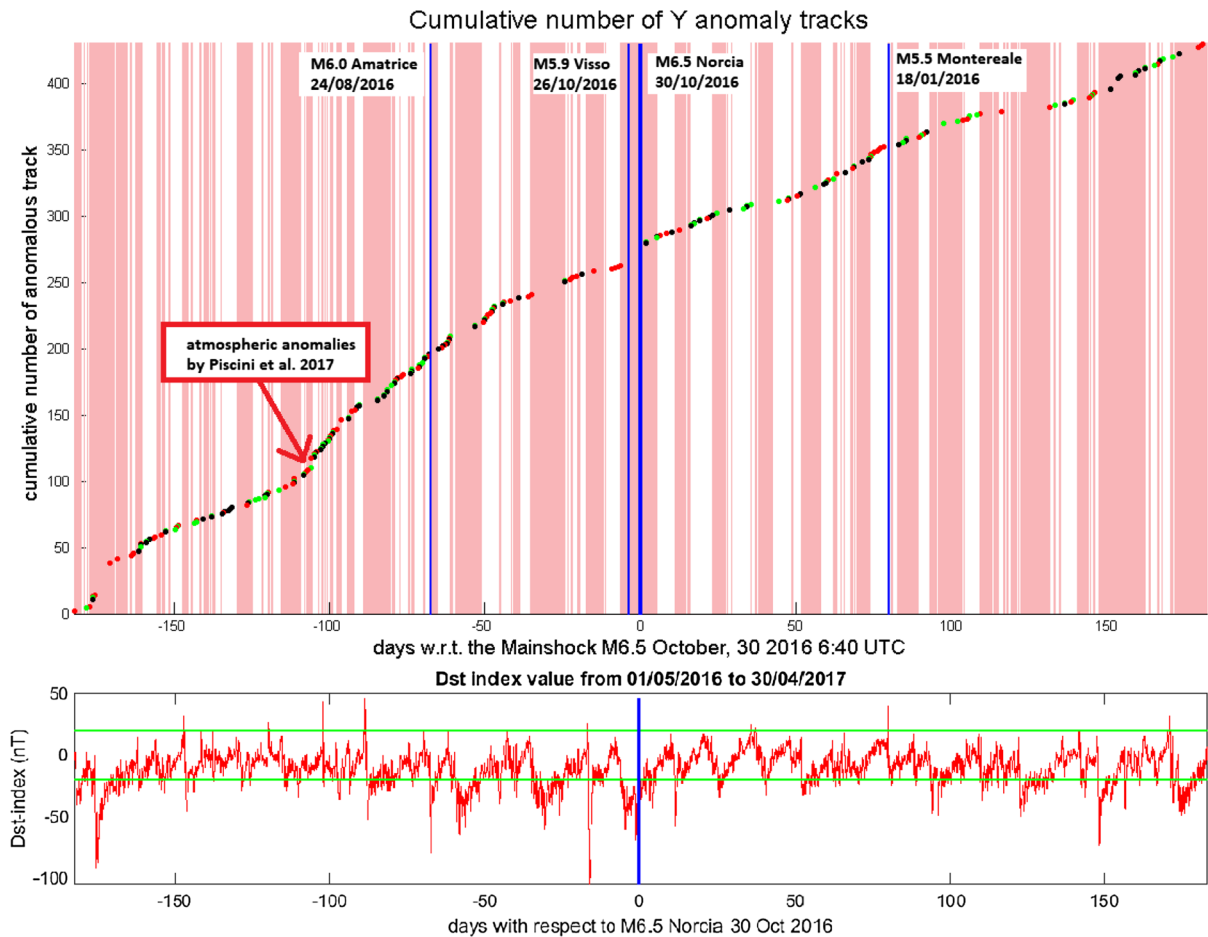


Figure 9

Cumulative number of Swarm three satellites anomalous tracks in Y component of magnetic field. The period from 01/05/2016 to 30/04/2017 has been investigated by thresholds in rms and frequency content (see text for details). During the disturbed hours, the cumulative graph is incremented by the same slope of the surrounding period. The red vertical bars represent the geomagnetic disturbed time ($IDstl > 20$ nT and/or $a_p > 10$ nT). The color of the dots indicates the satellite that detects the anomaly: black for Alpha, red for Bravo and green for Charlie. The blue vertical lines depict the main earthquakes in the seismic sequence. Bottom graph represents the Dst value for the same period; the upper and lower green lines are the thresholds within we define the quiet geomagnetic time (together with the $a_p \leq 10$ nT)

most of energy of the green circle anomaly shown by Fig. 3 is concentrated between about 40 and 60 s (see red rectangle in Fig. 8).

To check the relationship between this anomaly with the seismic activity in Central Italy we perform a blind research extracting all the anomalies with similar characteristics defined by a threshold k_t over the root mean square (rms) of the residual inside a 1 degree latitude window compared with the root mean square of the whole track ($l_{geomagnetic\ latitude} \leq 50^\circ$). The mean energy in the periods between 40 and 60 s is investigated in Fig. 8 (the

candidate track) and it reaches 0.048 (nT/s)². So, we define a second threshold over this energy equal to 0.040 (nT/s)². All tracks are analysed, both during daytime and nighttime, as the algorithm compares the investigated windows with the whole track so the local time dependence of background does not influence our technique.

Figure 9 shows the cumulative number of Swarm three satellites anomalous tracks in Y component of magnetic field. The period from 01/05/2016 to 30/04/2017 is investigated by a threshold k_t equal to 1.75 in rms and a threshold of 0.040 (nT/s)² in energy

content in the periods between 40 and 60 s. The tracks are tagged as anomalous only during geomagnetically quiet time defined by thresholds over Dst and a_p ($IDstl \leq 20$ nT and $a_p \leq 10$ nT), to avoid solar disturbance of ionosphere. In Fig. 9 the geomagnetic disturbed time ($IDstl > 20$ nT or $a_p > 10$ nT) is underlined by vertical red bars. Each point of the cumulate of this figure corresponds to an anomalous track of one of the three Swarm satellites (black Alpha, red Bravo and green Charlie). The origin times of the main earthquakes (i.e. M5.5+) of the seismic sequence are presented as vertical blue lines with close explanation label. The cumulative graph is made creating a curve that starts from 0 and, when we detect an anomaly, we add (i.e. cumulate) one unit to the previous value. As it is a sum of positive quantities, it is always a monotone increasing.

As during disturbance time we do not select anomalous tracks, this selection could influence the pattern of the cumulative number of the anomalous track over the time. To avoid this, the cumulative number is increased during the disturbed hours by the same slope that has outside in the same period. This allows us to interpret better the shape of the cumulative graph without introducing artificial variations of slope due to not analysed periods (for geomagnetic disturbance and/or storms).

Without special phenomena, we expect that the cumulative number of anomalies increases linearly with the time, so we search for periods when there is some deviation from the linearity of this curve and we investigate them.

The general shape of the cumulative number of anomalous tracks so constructed (Fig. 9) shows an increase starting about 40 days before the M6.0 24/08/2016 Amatrice earthquake. The trace comes back to the previous slope about 23 days after the same earthquake, so we suppose that this is the typical slope of this graph (i.e. the slope without seismic events).

What is very interesting is that the starting time of slope-variation of the cumulative number of the anomalous tracks coincides and follows the anomalies in skin temperature (skt), total column water vapour (tcwv) and total column ozone (tco3) found by Piscini et al. (2017) between 11 and 15 July 2016.

The synchronism between these parameters and the time sequence (first, the surface or close surface variations of skt and tcwv, then tco3 and finally the ionospheric disturbance) could confirm a possible perturbation coming from lithosphere up to ionosphere.

Finally, we check the number of anomalies at different times of the analysed period. The total number of the anomalous Swarm (Alpha, Bravo and Charlie) tracks in the geomagnetically quiet analysed time is 260 (Alpha 84, Bravo 94 and Charlie 82). Before the 24 August 2016 the number of anomalous tracks is 117 (over 812 analysed tracks in geomagnetically quiet conditions). Between M6.0 Amatrice 24 August 2016 earthquake and Norcia M6.5 30 October 2016 earthquake, the number of anomalous tracks is 43 (over 351 quiet tracks) and after the M6.5 main shock the number of anomalous tracks is 100 (over 1238), so the percentage of anomalous tracks is 14.4% before M6.0 EQ, 12.3% between M6.0 EQ and M6.5 EQ and 8.1% after the mainshock. The greater percentage of anomalous tracks before the two principal seismic events of the sequence confirms the reliability of this method to search for possible seismic source geomagnetic anomalies in Swarm satellite data.

6. Discussion and Conclusions

Among all the shown tracks, the most interesting one is represented in Fig. 3: the geomagnetic conditions are very quiet and there is a clear anomaly in the Y component not presenting anomalies on the other components (as Fig. 2), strengthening the hypothesis of a possible lithospheric origin for this anomaly. The anomalies shown in Figs. 2 and 7 are, instead, likely related to the auroral geomagnetic activity. Note that these latter anomalies, probably due to external geomagnetic activity, affect the three components of magnetic field, instead the anomaly in green circle of Fig. 3 is present only in Y component of geomagnetic field suggesting a different nature of this anomaly. Furthermore, the possibility to detect Earth—internal source of anomalies in Y-component is higher than in other two components as it is less affected by external perturbations (Pinheiro et al. 2011).

The possibility of perturbation in ionosphere electromagnetic environment was statistically demonstrated in DEMETER satellite data by Li and Parrot (2013) and some most recent works (Yan et al. 2017; Ho et al. 2018). The detected anomaly in Swarm magnetic data is compatible with anticipation time with respect to M6.0 24 August 2016 Amatrice earthquake found in these works and also the earthquake magnitude is inside the different range that the authors used for their statistical analysis.

In Fig. 6, it appears a very peculiar pattern that can be candidate for an earthquake precursor, but, unfortunately, the geomagnetic conditions are not sufficiently calm to claim any conclusions about this effect and its possible association with the lithospheric activity, even if suggested by the later phenomena. Therefore, a LAIC for this phenomenon is very difficult to prove. The pattern could be due to a passage of particles, but these could have been introduced from the outside (e.g. solar wind) rather than from the lithosphere.

Due to the peculiarity and the exclusion of other phenomena, the signal acquired by Swarm Charlie 3.2 days before the start of the whole seismic sequence is an excellent candidate as a magnetic seismic precursor. This is further confirmed by the blind research of anomalous signals in the satellite magnetic field, combining an automatic analysis in intensity and frequency of the signal to identify the anomalies. The combined use of these methods was successfully demonstrated to be promising for searching possible electromagnetic seismic precursors (e.g. Wen et al. 2012). In our analysis, we find an increase of the cumulative number of anomalous tracks that immediately follows the surface–atmosphere perturbation found by Piscini et al. (2017).

The temporal sequence of the different anomalies seems to confirm the Lithosphere–Atmosphere–Ionosphere coupling mechanism, perturbing firstly the surface and near surface layers (through the quantities of skt , $tcwv$), then an intermediate upper atmospheric layer as evidenced by ozone and finally some days after, the upside ionosphere as found in the automatic analysis applied on Swarm magnetic data by the increase of the cumulative number of anomalies.

In summary, the anomalous track of Charlie of 20 August 2016 (i.e. 3.2 days before the start of the seismic sequence) seems to be a phenomenon of different nature (e.g. precipitation of particles), that could be linked to the imminent earthquake and, if it is confirmed in other case studies, could be useful as a “last alarm” in a future platform to predict earthquakes together with other ionosphere, ground and atmospheric observations.

Acknowledgements

This work was undertaken in the framework of the European Space Agency (ESA)-funded project SAFE (Swarm for Earthquake study) and Agenzia Italiana Spaziale (ASI) founded project LIMADOU-Science. The authors thank prof. F. Javier Pavón-Carrasco for the significant contribution to the development of Swarm data analysis software and the seismologist Dr. Rita Di Giovambattista for her very important suggestions provided during the preparation of the work. The Editor and an anonymous referee are greatly thanked for their important comments that helped us very much in improving the quality of the paper.

Publisher’s Note Springer Nature remains neutral with regard to jurisdictional claims in published maps and institutional affiliations.

REFERENCES

- Akhoondzadeh, M., De Santis, A., Marchetti, D., Piscini, A., & Cianchini, G. (2018). Multi precursors analysis associated with the powerful Ecuador (MW = 7.8) earthquake of 16 April 2016 using Swarm satellites data in conjunction with other multi-platform satellite and ground data. *Advances in Space Research*, 61(1), 248–263.
- De Santis, A., Balasis, G., Pavón-Carrasco, F. J., Cianchini, G., & Manda, M. (2017). Potential earthquake precursory pattern from space: The 2015 Nepal event as seen by magnetic Swarm satellites. *Earth and Planetary Science Letters*, 461, 119–126.
- De Santis, A., De Franceschi, G., Spogli, L., Perrone, L., Alfonsi, L., Qamili, E., et al. (2015). Geospace perturbations induced by the Earth: The state of the art and future trends. *Physics and Chemistry of the Earth*. <https://doi.org/10.1016/j.pce.2015.05.004>.

- Di Luccio, F., Ventura, G., Di Giovambattista, R., Piscini, A., & Cinti, F. R. (2010). Normal faults and thrusts reactivated by deep fluids: The 6 April 2009 Mw6.3 L'Aquila earthquake, central Italy. *Journal of Geophysical Research*, *115*, B06315.
- Dobrovolsky, I. P., Zubkov, S. I., & Miachkin, V. I. (1979). Estimation of the size of earthquake preparation zones. *Pure and Applied Geophysics*, *117*, 1025.
- Donner, R. V., Potirakis, S. M., Balasis, G., Eftaxias, K., & Kurths, J. (2015). Temporal correlation patterns in pre-seismic electromagnetic emissions reveal distinct complexity profiles prior to major earthquakes. *Physics and Chemistry of the Earth*. <https://doi.org/10.1016/j.pce.2015.03.008>.
- Fraser-Smith, A. C., Bernardi, A., McGill, P. R., Ladd, M. E., Helliwell, R. A., & Villard, O. G., Jr. (1990). Low-frequency magnetic field measurements near the behaviour of the Ms 7.1 Loma Prieta Earthquake. *Geophysical Research Letters*, *17*(9), 1465–1468.
- Freund, F. (2011). Pre-earthquake signals: Underlying physical processes. *Journal of Asian Earth Sciences*, *41*, 383–400.
- Freund, F. (2013). Earthquake forewarning—A multidisciplinary challenge from the ground up to space. *Acta Geophysica*, *61*(4), 775–807.
- Freund, F. T., Takeuchi, A., Lau, B. W. S., Al-Manaseer, A., Fu, C. C., Bryant, N. A., et al. (2007). Stimulated infrared emission from rocks: assessing a stress indicator. *eEarth*, *2*, 1–10.
- Friis-Christensen, E., Lühr, H., & Hulot, G. (2006). Swarm: A constellation to study the Earth's magnetic field. *Earth Planets Space*, *58*, 351–358.
- Grayver, A. V., Schnepf, N. R., Kuvshinov, A. V., Sabaka, T. J., Manoj, C., & Olsen, N. (2016). Satellite tidal magnetic signals constrain oceanic lithosphere–asthenosphere boundary. *Science Advances*. <https://doi.org/10.1126/sciadv.1600798>.
- Hattori, K. (2004). ULF geomagnetic changes associated with large earthquakes. *Terrestrial Atmospheric and Oceanic Sciences*, *15*(3), 329–360.
- Hayakawa, M. (2015). *Earthquake prediction with radio techniques*. Singapore: J. Wiley & Sons.
- Ho, Y.-Y., Jhuang, H.-K., Lee, L.-C., & Liu, J.-Y. (2018). Ionospheric density and velocity anomalies before $M \geq 6.5$ earthquakes observed by DEMETER satellite. *Journal of Asian Earth Sciences*, *166*, 210–222.
- Irrgang, C., Saynisch, J., & Thomas, M. (2017). Utilizing oceanic electromagnetic induction to constrain an ocean general circulation model: A data assimilation twin experiment. *Journal of Advances in Modeling Earth Systems*, *9*, 1703–1720.
- Kikuchi, T., Lühr, H., Schlegel, K., Tachihara, H., Shinohara, M., & Kitamura, T.-I. (2000). Penetration of auroral electric fields to the equator during a substorm. *Journal of Geophysical Research*, *105*(A10), 23251–23261.
- Knudsen, D. J., Burchill, J. K., Buchert, S. C., Eriksson, A. I., Gill, R., Wahlund, J.-E., et al. (2017). Thermal ion imagers and Langmuir probes in the Swarm electric field instruments. *Journal of Geophysical Research: Space Physics*, *122*, 2655–2673.
- Kuo, C. L., Huba, J. D., Joyce, G., & Lee, L. C. (2011). Ionosphere plasma bubbles and density variations induced by pre-earthquake rock currents and associated surface charges. *Journal of Geophysical Research*, *116*, A10317.
- Kuo, C. L., Lee, L. C., & Huba, J. D. (2014). An improved coupling model for the lithosphere–atmosphere–ionosphere system. *Journal of Geophysical Research: Space Physics*, *119*, 3189–3205.
- Léger, J.-M., Jager, T., Bertrand, F., Hulot, G., Brocco, L., Vigneron, P., et al. (2015). In-flight performance of the absolute scalar magnetometer vector mode on board the Swarm satellites. *Earth, Planets and Space*. <https://doi.org/10.1186/s40623-015-0231-1>.
- Li, M., & Parrot, M. (2013). Statistical analysis of an ionospheric parameter as a base for earthquake prediction. *Journal of Geophysical Research: Space Physics*, *118*(6), 3731–3739.
- Lück, C., Kusche, J., Rietbroek, R., & Löcher, A. (2018). Time-variable gravity fields and ocean mass change from 37 months of kinematic Swarm orbits. *Solid Earth*, *9*, 323–339.
- Marchetti, D., & Akhoondzadeh, M. (2018). Analysis of Swarm satellites data showing seismo-ionospheric anomalies around the time of the strong Mexico (Mw = 8.2) earthquake of 08 September 2017. *Advances in Space Research*. <https://doi.org/10.1016/j.asr.2018.04.043>.
- Molchanov, O. A., Kopytenko, Yu A., Voronov, P. M., Kopytenko, E. A., Matiashvili, T. G., Fraser-Smith, A. C., et al. (1992). Results of ULF magnetic field measurements near the epicenters of the Spitak (Ms = 6.9) and Loma Prieta (Ms = 7.1) earthquakes: Comparative analysis. *Geophysical Research Letters*, *19*(14), 1495–1498.
- Olsen, N., Friis-Christensen, E., Floberghagen, R., et al. (2013). The Swarm satellite constellation application and research facility (SCARF) and Swarm data products. *Earth Planet Space*. <https://doi.org/10.5047/eps.2013.07.001>.
- Olsen, N., Hulot, G., & Sabaka, T. J. (2010). Measuring the Earth's magnetic field from space: Concepts of past, present and future missions. *Space Science Reviews*, *155*, 65–93.
- Olsen, N., Ravat, D., Finlay, C. C., & Kother, L. K. (2017). LCS-1: A high-resolution global model of the lithospheric magnetic field derived from CHAMP and Swarm satellite observations. *Geophysical Journal International*, *211*(3), 1461–1477.
- Pinheiro, K. J., Jackson, A., & Finlay, C. C. (2011). Measurements and uncertainties of the occurrence time of the 1969, 1978, 1991, and 1999 geomagnetic jerks. *Geochemistry, Geophysics, Geosystems*, *12*, Q10015.
- Piscini, A., De Santis, A., Marchetti, D., & Cianchini, G. (2017). A multi-parametric climatological approach to study the 2016 Amatrice-Norcia (Central Italy) earthquake preparatory phase. *Pure and Applied Geophysics*, *174*(10), 3673–3688.
- Pulinets, S., & Boyarchuk, K. (2004). *Ionospheric precursors of earthquakes*. New York: Springer.
- Pulinets, S., & Ouzounov, D. (2011). Lithosphere–atmosphere–ionosphere coupling (LAIC) model—An unified concept for earthquake precursors validation. *Journal of Asian Earth Sciences*, *41*(4–5), 371–382.
- Ritter, P., Lühr, H., & Rauberg, J. (2013). Determining field-aligned currents with the Swarm constellation mission. *Earth, Planets and Space*. <https://doi.org/10.5047/eps.2013.09.006>.
- Thébault, E., et al. (2015). International geomagnetic reference field: The 12th generation. *Earth Planets Space*. <https://doi.org/10.1186/s40623-015-0228-9>.
- Tinti, E., Scognamiglio, L., Michelini, A., & Cocco, M. (2016). Slip heterogeneity and directivity of the ML 6.0, 2016, Amatrice earthquake estimated with rapid finite-fault inversion. *Geophysical Research Letters*. <https://doi.org/10.1002/2016GL071263>.

- Wen, S., Chen, C.-H., Yen, H.-Y., Yeh, T.-K., Liu, J.-Y., Hattori, K., et al. (2012). Magnetic storm free ULF analysis in relation with earthquakes in Taiwan. *Natural Hazards and Earth System Sciences*, 12, 1747–1754.
- Yan, R., Parrot, M., & Pinçon, J.-L. (2017). Statistical study on variations of the ionospheric ion density observed by DEMETER and related to seismic activities. *Journal of Geophysical Research: Space Physics*. <https://doi.org/10.1002/2017JA024623>.

(Received September 29, 2018, revised February 14, 2019, accepted February 18, 2019, Published online February 25, 2019)